Tension Gauge Tethers as tension-dependent lifetime sensors

Jingzhun Liu,[1] Shimin Le,[2] Mingxi Yao,[3] Wenmao Huang,[2] Zhikai Tio,[4] Yu Zhou,[1] and Jie Yan[1,2,*]

[1] *Mechanobiology Institute, National University of Singapore, Singapore 117411*
[2] *Department of Physics, National University of Singapore, Singapore 117546*
[3] *Department of Biomedical Engineering, Southern University of Science and Technology, P. R. China 518055*
[4] *Department of Chemical and Biomolecular Engineering, National University of Singapore, Singapore 117585*

(Dated: March 11, 2022)

Mechanotransduction of cells, a time-taking process, relies on responding to tension transmitted along various supramolecular linkages. The minimal lifetimes of the linkages needed for proper mechanotransduction remain poorly understood. We propose that such information can be provided using tension-dependent lifetime sensors that undergo irreversible tension-dependent dissociation. We quantified the tension-dependent lifetime of DNA-based Tension Gauge Tethers. Comparing it with the observations from previous cell studies, the minimal lifetime of individual integrin-RGD linkage needed for cell spreading was determined to be tens of seconds over the physiological tension range.

PACS numbers: 87.14.gk, 87.15.-v, 87.15.He, 87.15.La, 87.80.-y

In cells, the actomyosin cytoskeleton network is linked to different cell membrane receptors and nuclear membrane proteins through sets of adaptor proteins. Some of the adhesive membrane receptors are further linked to extracellular matrix or neighboring cells, by which the cells in tissues are physically linked via cell-matrix and cell-cell adhesions [1–5]. Due to actomyosin contraction or external mechanical perturbations, dynamic tension is generated and transmitted along various intra/intercellular supramolecular linkages. By responding to the level of tension transmitted along such supramolecular linkages, cells are able to sense and respond to the mechanical cues in the local environment through processes referred to as mechanosensing and mechanotransduction, which play crucial roles in regulation of various cell behaviours including cell spreading, cell migration, cell differentiation, growth and tissue repair [1–10].

As mechanotransduction is a process that takes time, under physiological level of tension, a mechanosensing supramolecular linkage needs to survive a certain lifetime to support these processes. However, this piece of important information has been largely missing from previous experimental investigations. We reason that such information can be provided using tension-dependent lifetime sensors, molecular complexes that undergo irreversible dissociation with well calibrated tension-dependent lifetimes $\tau(f)$. Such molecular complexes of different tension-dependent lifetime sensors inserted into a mechanosensing supramolecular linkage can report the minimal lifetime scale needed for the proper mechanotransduction associated with the linkage.

Tension Gauge Tethers (TGTs), short double-stranded DNA (dsDNA) segments that undergo tension-dependent irreversible strand dissociation, can fulfil this purpose. TGTs were originally developed as extracellular tension sensors to report tension level based on an assumption that the strand dissociation requires tension exceeding a certain threshold termed the tension tolerance [11]. Here, we repurpose the applications of TGTs for reporting the minimal lifetimes of extracellular mechanosensing supramolecular linkages needed for proper mechanotransduction (Fig. 1).

We designed a single-molecule detector (Fig. 2(a)), consisting of a DNA hairpin construct spanned between two single-stranded DNA (ssDNA) handles, and an ssDNA oligo that is complementary to regions of both ssDNA handles adjacent to the fork of the hairpin marked by green and red, respectively. The red duplex is the target to be measured for its mechanical stability. When the red duplex is ruptured at a tension slightly greater than the threshold detabilizing-tension of the hairpin (typically greater than 10 piconewtons (pN)), it will lead to a large stepwise increase in the height of the bead that can be detected by our in-house constructed magnetic tweezers. The technical details of the magnet tweezers can be found in our previous publications [12, 13]. Further details on the manipulation of the single-molecule detector can be found in Supplemental Material I-IV [14] . The green duplex is made much longer than the red duplex to ensure that the rupturing transition only occurs on the red duplex (Supplemental Material V [14]). After rupturing the red duplex, the ssDNA oligo remains stably bound to the detector via the green duplex (Fig. 2(a), right), which allows the red duplex to quickly reform when tension is reduced to below the hairpin unzipping threshold tension. This way, many data points can be obtained from one detector.

We quantified the tension-dependent rupturing probability of the red duplex over a time interval Δt when it was held at a constant tension F, $p_F(\Delta t)$. The average lifetime of the red duplex $\tau(f)$ was obtained by fitting $p_F(\Delta t)$ data with a single-exponential function

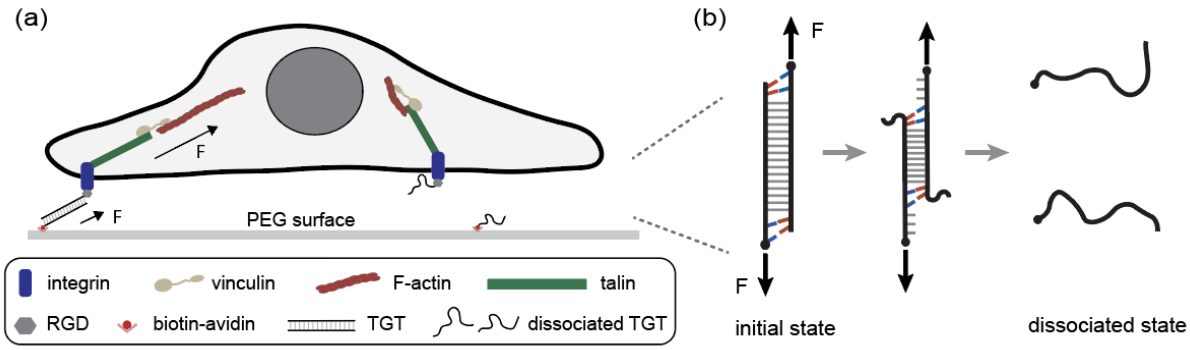

Fig. 1. TGTs as a tension-dependent lifetime sensor. (a) Schematics of a cell adhered to a surface mediated by integrins binding to RGDs tethered to the surface via TGTs. When the two strands in a TGT dissociate, the corresponding tension-transmission pathway disappears. (b) Illustration of the tension-dependent strand dissociation pathway of a TGT via strand-peeling from the ends [15]. The force attaching points are indicated by the black circles at the end of the DNA strands.

$1 - e^{(-\Delta t/\tau)}$. The $p_F(\Delta t)$ data were obtained by applying tension-jump cycles described in Figure 2(b). Each tension-jump cycle starts with a tension, F_l, at which the hairpin is stable, for one minute to allow the red duplex to form. In the subsequent step, tension is jumped to F_d which is slightly higher than the hairpin unzipping threshold tension, for two seconds to check whether the red duplex is formed. The two states of the red strand, hybridized or ruptured, can be unambiguously determined by their large extension difference (Fig. 2(a)). Then, the tension is jumped to a target higher tension F, for a holding time of Δt, during which the red duplex may or may not rupture. Repeating the tension-jump cycles for multiple times, $p_F(\Delta t)$ is calculated as the number of cycles where the red duplex is ruptured, N_r, divided by the total number of cycles, N (i.e., $p_F(\Delta t) = N_r/N$).

Most of cell studies have been performed at the human body temperature of 37 °C [11, 16–23]. As $\tau(f)$ of a TGT is highly sensitive to temperature (Supplemental Material VI [14]), we quantified $\tau(f)$ of four TGTs (Table I) at 37 °C, including three (7-bp, 11-bp and 15-bp) widely used in previous studies and one modified (13-bp) from the 15-bp TGT. For each TGT, repeating the tension-jump cycles for multiple tethers ($N = 10$), the $p_F(\Delta t)$ data was determined from at least 50 cycles at each holding time. Figure 3(a)-(c) shows $p_F(\Delta t)$ obtained from three TGTs, a 15-bp TGT and an 11-bp TGT used in previous cell studies [11], as well as a 13-bp TGT generated by deleting the last two base pairs of the 15-bp TGT. The $p_F(\Delta t)$ curves of the three TGTs obtained at the same forces shift left as the lengths of TGTs decrease (Fig. 3(d)), suggesting decreased mechanical stability of shorter TGTs.

For each TGT, the best-fitted lifetime was obtained over a certain tension range (Fig. 4(a)), with the errors obtained by bootstrap analysis (Supplemental Material VII [14]). Outside the tension range, the lifetime of the TGT is either too short or too long to be accurately determined (Supplemental Material VIII [14]). Therefore, $\tau(f)$ is extrapolated (solid line, Fig. 4(a)) from the measured $\tau(f)$ data to tensions outside the range of measurement based on an expression derived from Arrhenius law of transition kinetics, $\tau(f) = \tau_0 e^{(-(\sigma(n^*)f - \eta(n^*)\sqrt{f})/k_BT)}$, where $\sigma = n^*(l_{1ss} - l_{1ds})$, and $\eta = n^* l_{1ss}\sqrt{(k_BT/A)}$ (Supplemental Material IX [14]). Here, $l_{1ss} = 0.7$ nm and $l_{1ds} = 0.34$ nm are the contour length of one nucleotide step of ssDNA and one base pair step of dsDNA, respectively, and $A = 0.7$ nm is the bending persistence length of ssDNA in 150 mM KCl [24, 25]. This model can be applied at tensions greater than a few pN where the worm-like chain polymer model of ssDNA is valid [26, 27].

TABLE I: Sequences of TGTs [11]

Length	Sequence (5' → 3')
7	GTG TCG T
11	GTG TCG TGC CT
13	GTG TCG TGC CTC C (truncated from # 15)
15	GTG TCG TGC CTC CGT

At the physiological range of tension from a few pN to 15 pN of individual integrin-RGD complex [28–30], the lifetime ranges for the three TGTs were determined to be $10^3 - 10^4$ s for the 15-bp TGT, $10^2 - 10^3$ s for the 13-bp TGT, and tens of seconds $10^1 - 10^2$ s for the 11-bp TGT. $\tau(f)$ for the 7-bp TGT in Table I is too short to be determined, which is $\ll 0.3$ s at physiological tension range (Supplemental Material VIII [14]).

The tension range in a mechanosensing supramolecular linkage depends on tension-dependent unfolding and refolding of tension-bearing domains in the linkage. During cytoskeleton network contraction where unfolded and

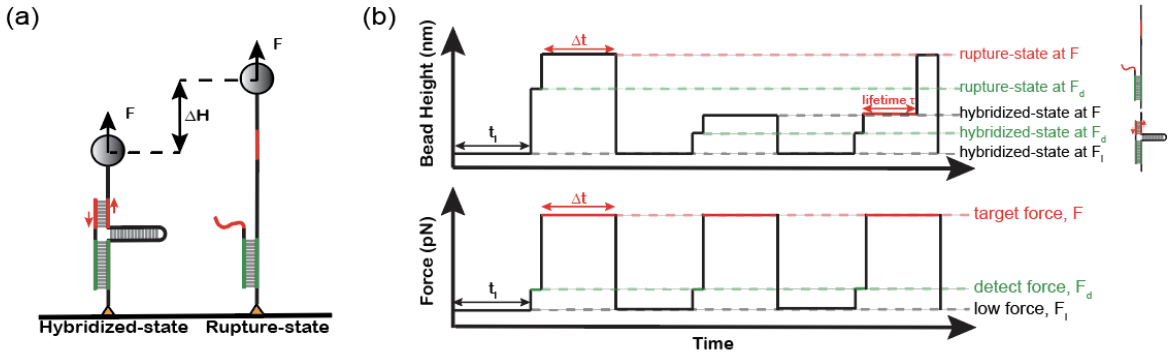

Fig. 2. Tension-jump cycles to quantify the mechanical stability of a TGT. (a) Schematic of the designed DNA detector tethered between a glass surface and a superparamagnetic bead. The TGT is shown in red. The green DNA duplex is to anchor the ssDNA on the detector for higher experimental throughput. (b) Schematics of tension-jump cycle applied to measure the lifetime of the TGT. The state of the TGT is determined based on the bead height.

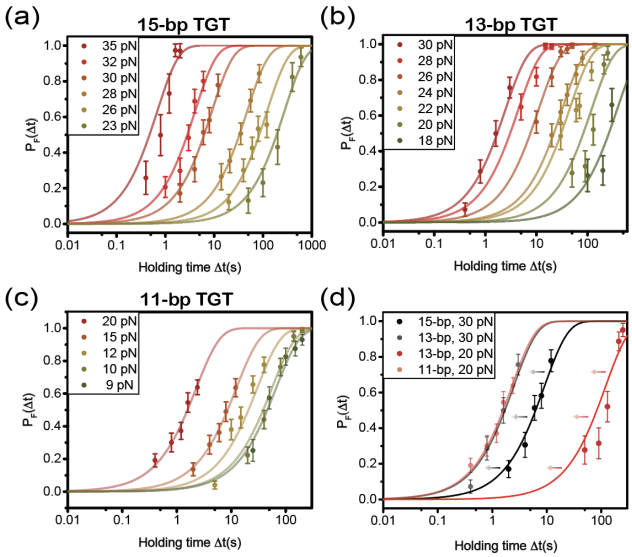

Fig. 3. Tension-dependent lifetimes of three TGTs in Table I at 37 °C. The probabilities of 15-bp TGT (a), 13-bp truncated TGT (b), and 11-bp TGT (c) rupturing within different holding times were detected over a certain tension range. (d) Comparison of the $p_F(\Delta t)$ curves of 15-bp and 13-bp TGTs at 30 pN (dark and light black line) and 13-bp and 11-bp TGTs at 20 pN (dark and light red line). (mean ± standard error).

folded domains co-exist, the tension is buffered within a typical range below 10 pN [31, 32]. During long range of cytoskeleton contraction that causes unfolding of all the tension-bearing domains, the tension level increases as further contraction occurs until the breakage of the linkage due to tension-dependent dissociation of protein-protein connections in the linkage. Figure 4(b) shows the probability of tensions at which the two strands of the three TGTs dissociate at different force-loading rates calculated from $\tau(f)$ by the equation $\rho(F) = \frac{1}{\tau(F)r} exp(-\int_0^F -\frac{1}{\tau(f)r} df)$ [33]. For the 11-bp TGT that provides the minimal stability to support mechanotransduction, the peak strand dissociation tension is in the range from 15 pN to 25 pN for loading rates over a physiologically relevant range from 1 pN/s to 10 pN/s (Supplemental Material X [14]).

We have examined the tension-dependent lifetimes, $\tau(f)$, of several TGTs. The quantity of $\tau(f)$ provides a full description of the mechanical stability of TGTs, from which the mechanical responses under various mechanical constraints, such as time-varying tension, can be derived. The three calibrated TGTs at 37 °C cover a wide range of mechanical stability that can be used in a broad range of experiments.

Up to now, the mechanical properties of TGTs have been described by a quantity called DNA tension tolerance, which is defined as the tension needed to separate the two DNA strands [11]. Based on this quantity, TGTs have been used as a tension sensor to report the whether tension exceeds a certain threshold. The tension tolerance of the TGTs has been estimated by deGennes' formula, an analytical expression that states a relationship between the critical tension making the DNA base pair unstable and the DNA length [34]. The derivation was based on static analysis of the elastic energy of the DNA, which does not consider the effects of thermal fluctuation of DNA at finite temperature [34] that can cause DNA strand dissociation of a short TGT at any tension within any time interval. Therefore, only under conditions (e.g., a sufficiently long DNA) when a TGT has a long lifetime comparable to the time scale involved in cell studies, tension tolerance may be approximated as a tension threshold for the strand dissociation.

However, our tension-dependent lifetime measurements (Fig. 4(a)) show that the three tested TGTs have

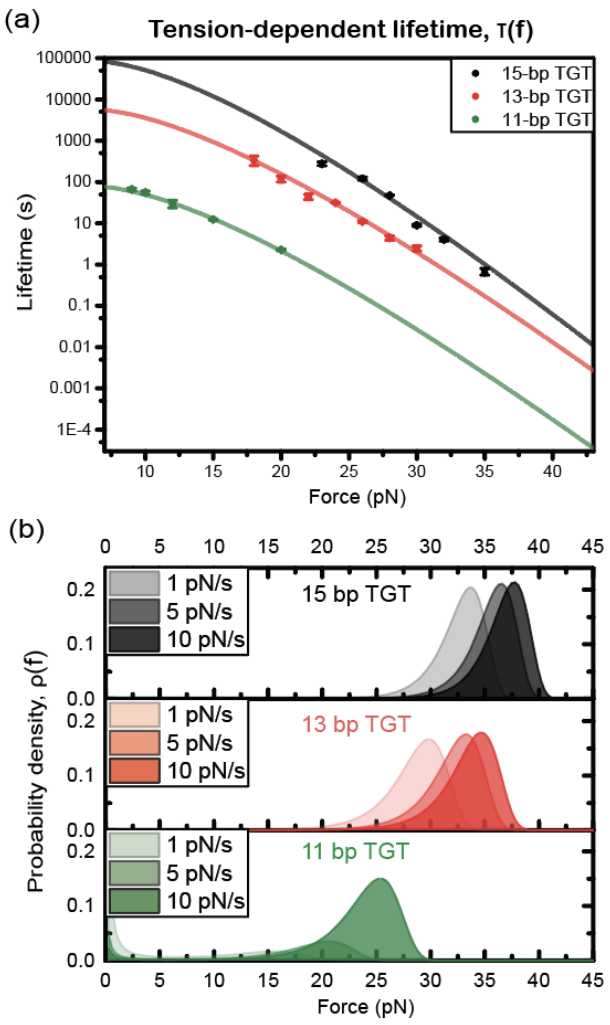

Fig. 4. The mechanical properties of TGTs in Table I. (a) The tension-dependent lifetime, $\tau(F)$, data is obtained from exponential fitting of measured $p_F(\Delta t)$ and is further extrapolated to tensions above a few pN using the structural-elastic model (Supplemental Material IX [14]). (b) The probability density of TGTs rupturing force under forces with different loading rates: 1 pN/s, 5 pN/s, and 10 pN/s, obtained from $\tau(f)$ of the corresponding TGTs.

an ultra-short lifetime at the tensions corresponding to the reported tension tolerances. At the reported tension tolerance of 43 pN [11], the 11-bp TGT has an ultra-short lifetime in the order of 10^{-3} s. Similarly, at the reported tension tolerance of 54 pN [11], the 15-bp TGT has an ultra-short lifetime in the order of 10^{-5} s. Even at tensions more than 15 pN below the predicted tension tolerances, the lifetimes are still shorter than one second. We can also investigate the problem from another point of view by considering the tensions at which the strand dissociation occurs when force increases under a certain loading rate. For both the 11-bp and 15-bp TGTs, the predicted distributions of TGT rupturing tensions are more than 15 pN below the reported tension tolerance value. Since mechanotransduction is a process that requires sufficiently long time for tension-dependent protein-protein interactions, these TGTs cannot report the tension threshold needed for the corresponding mechanotransduction processes based on their reported tension tolerance values. Hence, the experimental observations from previous cell studies reporting tension levels based on TGTs' tension tolerance values require a different interpretation. It also raises an important question on what information provided from these TGTs in previous cell studies.

In our view, the important information provided by these short TGTs is the time scale of a mechanosensing supramolecular linkage needed for proper mechanotransduction at the physiological level of tensions. It has been reported that the tensions transmitted across integrin-RGD are in the order of several pN reported using DNA hairpin tension sensors [35, 36]. Unlike TGTs, DNA hairpin tension sensors undergo reversible unzipping and rezipping transitions. Therefore, a threshold tension can be defined at which the two states have equal probabilities. Similar tension range was reported for the talin-mediated tension-transmission from integrin to cytoskeleton network over a range from a few pN to about 12 pN using intracellular tension sensors, a calibrated polypeptide inserted into a protein in the tension-transmission supramolecular linkages [37, 38]. Over such physiological tension range, the 11-bp TGT has a lifetime of tens of seconds at tensions < 12 pN at 37 °C (Fig. 4(a)). Hence, the result from the previous cell study showing that TGTs with tension tolerances of 43 pN (the 11-bp TGT in Table I) or higher were needed for the formation of matured cell-matrix adhesions [11] can be reinterpreted as that a minimal lifetime of individual integrin-RGD complexes, tens of seconds at tensions of a few pN, is needed for proper integrin-based mechanotransduction for cell-matrix adhesion.

To summarise, most of previous works were focused on reporting the tension level, whereas the minimal lifetime of the linkage needed for mechanotransduction at the physiological level of tensions remains poorly understood. We show that TGTs can be repurposed as highly useful extracellular minimal lifetime sensors. According to similar principle, intracellular minimal lifetime sensors can be designed based on the complexes formed with small protein domains inserted into a mechanosensing supramolecular linkage, which undergo irreversible dissociation with well calibrated tension dependent lifetimes.

ACKNOWLEDGEMENTS

We thank Alexander Bershadsky and Pakorn Tony Kanchanawong for critical reading of the manuscript. The research was funded by the Singapore Ministry of Education Academic Research Funds Tier 2 (MOE2019-T2-1-099, MOE-T2EP50220-0015) and the Ministry of Education under the Research Centres of Excellence programme.

AUTHOR CONTRIBUTIONS

J.L. and J.Y. designed the research, interpreted the experimental data and wrote the manuscript. J.L. and Z.T., carried out the single-molecule experiments and performed data analysis. J.L., S.L., M.Y., Y.Z., and W.H. contributed to the design and synthesized the DNA detector for single-molecule experiments. J.Y. supervised the research.

* Email: phyyj@nus.edu.sg

[1] T. Iskratsch, H. Wolfenson, and M. P. Sheetz, Nature reviews Molecular cell biology **15**, 825 (2014).

[2] C. Uhler and G. Shivashankar, Nature reviews Molecular cell biology **18**, 717 (2017).

[3] K. H. Vining and D. J. Mooney, Nature reviews Molecular cell biology **18**, 728 (2017).

[4] T. Panciera, L. Azzolin, M. Cordenonsi, and S. Piccolo, Nature reviews Molecular cell biology **18**, 758 (2017).

[5] B. Ladoux and R.-M. Mège, Nature reviews Molecular cell biology **18**, 743 (2017).

[6] Z. Sun, S. S. Guo, and R. Fässler, Journal of Cell Biology **215**, 445 (2016).

[7] I. Schoen, B. L. Pruitt, and V. Vogel, Annual Review of Materials Research **43**, 589 (2013).

[8] A. Angulo-Urarte, T. van der Wal, and S. Huveneers, Biochimica et Biophysica Acta (BBA)-Biomembranes **1862**, 183316 (2020).

[9] M. Michael and M. Parsons, Current opinion in cell biology **63**, 31 (2020).

[10] F. Martino, A. R. Perestrelo, V. Vinarskỳ, S. Pagliari, and G. Forte, Frontiers in physiology **9**, 824 (2018).

[11] X. Wang and T. Ha, Science **340**, 991 (2013).

[12] H. Chen, H. Fu, X. Zhu, P. Cong, F. Nakamura, and J. Yan, Biophysical Journal **100**, 517 (2011).

[13] X. Zhao, X. Zeng, C. Lu, and J. Yan, Nanotechnology (2017).

[14] See Supplemental Material at [URL will be inserted by publisher] for detailed information of magnetic-tweezer experiment, base pair-destablizing tension, temperature-sensitive mechanical stability of TGTs, bootstrap sampling methods, structural-elastic model, and the physiologically relevant tension range.

[15] S. Cocco, J. Yan, J.-F. Léger, D. Chatenay, and J. F. Marko, Physical Review E **70**, 011910 (2004).

[16] F. Chowdhury, I. T. Li, B. J. Leslie, S. Doğanay, R. Singh, X. Wang, J. Seong, S.-H. Lee, S. Park, N. Wang, *et al.*, Integrative Biology **7**, 1265 (2015).

[17] M. H. Jo, W. T. Cottle, and T. Ha, ACS Biomaterials Science & Engineering **5**, 3856 (2018).

[18] Y. Zhang, Y. Qiu, A. T. Blanchard, Y. Chang, J. M. Brockman, V. P.-Y. Ma, W. A. Lam, and K. Salaita, Proceedings of the National Academy of Sciences **115**, 325 (2018).

[19] Y. Zhao, A. Sarkar, and X. Wang, Biosensors and Bioelectronics **150**, 111959 (2020).

[20] Y. Zhao, Y. Wang, A. Sarkar, and X. Wang, Iscience **9**, 502 (2018).

[21] Y. Zhao, K. Pal, Y. Tu, and X. Wang, Journal of the American Chemical Society **142**, 6930 (2020).

[22] Y. Hu, V. P.-Y. Ma, R. Ma, W. Chen, Y. Duan, R. Glazier, B. G. Petrich, R. Li, and K. Salaita, Angewandte Chemie **133**, 18192 (2021).

[23] H. Li, C. Zhang, Y. Hu, P. Liu, F. Sun, W. Chen, X. Zhang, J. Ma, W. Wang, L. Wang, *et al.*, Nature Cell Biology **23**, 642 (2021).

[24] S. Guo, Q. Tang, M. Yao, H. You, C.-H. Le, S., and J. Yan, Chemical science **9**, 5871 (2018).

[25] X. Zhang, H. Chen, S. Le, I. Rouzina, P. S. Doyle, and J. Yan, Proceedings of the National Academy of Sciences **110**, 3865 (2013).

[26] H. Fu, S. Le, C. Hu, K. Muniyappa, and Y. Jie, Nucleic Acids Research , 924 (2013).

[27] A. Bosco, J. Camunas-Soler, and F. Ritort, Nucleic Acids Research **42**, 2064 (2013).

[28] F. Li, S. D. Redick, H. P. Erickson, and V. T. Moy, Biophysical Journal **84**, 1252 (2003).

[29] E. Kokkoli, S. E. Ochsenhirt, and M. Tirrell, Langmuir the Acs Journal of Surfaces & Colloids **20**, 2397 (2004).

[30] E. L. Baker and M. H. Zaman, Journal of Biomechanics **43**, 38 (2010).

[31] M. Yao, B. T. Goult, B. Klapholz, X. Hu, C. P. Toseland, Y. Guo, P. Cong, M. P. Sheetz, and J. Yan, Nature communications **7**, 1 (2016).

[32] Shimin, Le, Miao, Yu, Ladislav, Hovan, Zhihai, Zhao, James, and Ervasti, Acs Nano (2018).

[33] Huijuan, You, Jingyuan, Wu, Fangwei, Shao, Jie, and Yan, Journal of the American Chemical Society **137**, 2424 (2015).

[34] Pierre-Gilles, de, and Gennes, Comptes Rendus De Lacadémie Des Sciences (2001).

[35] B. L. Blakely, C. E. Dumelin, B. Trappmann, L. M. McGregor, C. K. Choi, P. C. Anthony, V. K. Duesterberg, B. M. Baker, S. M. Block, D. R. Liu, *et al.*, Nature methods **11**, 1229 (2014).

[36] Y. Zhang, C. Ge, C. Zhu, and K. Salaita, Nature communications **5**, 1 (2014).

[37] M. D. Brenner, R. Zhou, D. E. Conway, L. Lanzano, E. Gratton, M. A. Schwartz, and T. Ha, Nano letters **16**, 2096 (2016).

[38] A. Kumar, M. Ouyang, K. Van den Dries, E. J. McGhee, K. Tanaka, M. D. Anderson, A. Groisman, B. T. Goult, K. I. Anderson, and M. A. Schwartz, Journal of Cell Biology **213**, 371 (2016).